







Comparison of the performance of a high voltage generator insulated by gas or liquid dielectric

Cite as: Rev. Sci. Instrum. **91**, 074712 (2020); <https://doi.org/10.1063/5.0009519>

Submitted: 01 April 2020 . Accepted: 06 July 2020 . Published Online: 22 July 2020

P. Antonini, E. Borsato, G. Carugno, F. Dal Corso , A. Facco , C. Fanin, C. S. Gallo , A. Galatá , R. Gobbo, L. La Torre, F. Montecassiano , M. Pegoraro, M. Poggi, and P. Zotto 





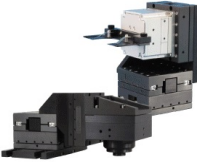
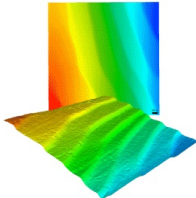
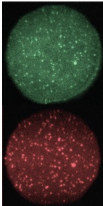
View Online



Export Citation



CrossMark

	<p>Nanopositioning Systems</p> 	<p>Modular Motion Control</p> 	<p>AFM and NSOM Instruments</p> 	<p>Single Molecule Microscopes</p> 
---	--	--	---	--

Comparison of the performance of a high voltage generator insulated by gas or liquid dielectric

Cite as: *Rev. Sci. Instrum.* **91**, 074712 (2020); doi: [10.1063/5.0009519](https://doi.org/10.1063/5.0009519)

Submitted: 1 April 2020 • Accepted: 6 July 2020 •

Published Online: 22 July 2020



View Online



Export Citation



CrossMark

P. Antonini,¹ E. Borsato,² G. Carugno,³ F. Dal Corso,³  A. Facco,¹  C. Fanin,³ C. S. Gallo,¹  A. Galatá,¹ 
R. Gobbo,⁴ L. La Torre,¹ F. Montecassiano,³  M. Pegoraro,³ M. Poggi,¹ and P. Zotto^{2,a)} 

AFFILIATIONS

¹INFN, Laboratori Nazionali di Legnaro, Viale dell' Università 2, Legnaro, 35020 Padova, Italy

²Università di Padova, Dipartimento di Fisica e Astronomia, Via Marzolo 8, 35131 Padova, Italy

³INFN, Sezione di Padova, Via Marzolo 8, 35131 Padova, Italy

⁴Università di Padova, Dipartimento di Ingegneria Industriale, Via Gradenigo 6A, 35131 Padova, Italy

^{a)} Author to whom correspondence should be addressed: Pierluigi.Zotto@unipd.it

ABSTRACT

A module of a wireless high voltage generator was tested immersed in both gaseous and liquid environments providing electrical insulation. The overall performance of the module as well as a detailed performance of the key components are reported, and a comparison between the results in gas and liquid is given. The tests performed on the liquid dielectric show that it is a valid alternative to high pressure gas electrical insulation.

Published under license by AIP Publishing. <https://doi.org/10.1063/5.0009519>

I. INTRODUCTION

Electrical insulation of any high voltage equipment can be assured by its immersion either in a gas or in an apolar liquid when solid dielectrics are not usable. Gas insulation is generally preferred in very high voltage generators, where electric/electronic or even mechanical (like in van de Graaff generators) components are used.

The main advantage favoring the use of a liquid is the possibility to avoid the use of high pressure gases, thus operating the generator at atmospheric pressure with an obvious reduction in safety risks. The setup of parasitic conduction leakage currents, is the main drawback in case a liquid is used. These currents are absent in gas and, in standard high voltage equipment, prevent from the control of the output voltage.

We developed a wireless high voltage generator^{1,2} consisting of several modules connected in series and that are remotely controllable. Electric power is supplied to each module by the conversion of continuous wave laser light, transported through quartz fibers, on photovoltaic cells.

Wireless high voltage generation is interesting since it is the only technology that allows series connection of modules, naturally forming a series of increasing high voltage gaps, thus, making an instrument easy to be upgraded and maintained: upgrading

can be done by increasing the number of generators and maintenance and repair can be performed on the bench while keeping the machine working by just replacing the defective module. Furthermore, it enables the independent control of any single module, thus obtaining better voltage stabilization. The wireless feature can be obtained either by light, as in our device, or by magnetic induction.^{3–5} The series connection and the use of light as the main power source allows both gases and liquids to be used as insulators, while the use of liquids is forbidden in induction generators, except for single gap ones like transformers, where a combination of solid and liquid insulation is used.⁶

Considering the advantages on the safety risk reduction and the easiness of operation brought by the use of a liquid insulator with respect to a gaseous one, we deeply investigated the pros and cons of both choices in order to base our decision on solid ground.

We have already presented a study⁷ on a carefully chosen dielectric liquid that is suitable for the use in this generator. The present paper reports on measurements performed on a fully equipped module operated while immersed in the aforementioned liquid and gas. Details of the global performance as well as of the performance of key components in both environments are given.

II. PERFORMANCE STUDIES

A simplified sketch of the module, highlighting the main components, is shown in Fig. 1: a series of GaAs solar concentration cells provide the power to a control board, which operates as the driver stage of a Cockcroft–Walton voltage multiplier; the multiplier output is stabilized by the control board via a 40 G Ω feedback resistive network that includes filter capacitors. A complete and detailed description of the module can be found in Ref. 2.

The purpose of our high voltage device is the generation of a uniform electrostatic field between two electrodes suitable for ion acceleration. The high voltage module of Fig. 1 is then packed between two aluminum electrodes of 20 cm radius, separated by a distance of 9 cm, and connected, respectively, to the lower and higher voltage potential terminals. Several such modules are then connected in series to form acceleration gaps.

Standard high voltage generators use high pressure gases as insulators, with liquid insulation used in some cases.⁸ It is evident that liquid insulation cannot be used if there are moving parts, like in a van de Graaff electrostatic machine, but also, in particular, liquid insulation can be envisaged only if the generator is serving a single gap. Otherwise, like in a multi-gap Cockcroft–Walton machine, the high voltage is distributed through the various gaps by a series of resistors and, therefore, any parasitic and undetected current inside the liquid prevents, by unpredictably modifying the voltage drop on the resistors, from an accurate voltage distribution.

We tried different options as insulating gases: N₂/CO₂ (80/20%) mixture, pure SF₆, and pure CO₂, operated at 0.2 MPa pressure. The liquid was inexpensive paraffin (Renoclean KU by Fuchs) which, from a chemical analysis shown in Fig. 2, composed mainly of tetradecane and decane with traces of other hydrocarbons. Preliminary studies were performed in order to determine the dielectric strength and resistivity of the liquid: the first was measured to be 11.2 kV/mm (according to IEC60156:1995 standard), to be compared with an average operation field of the device around 1.1 kV/mm, while the latter was non-ohmic, as shown in Fig. 3, but suitable for our needs.

The voltage multiplier and the feedback chain are completely covered by epoxy, while the control board and the solar cells are not topped and, therefore, their behavior could be affected by the insulation properties of the fluid in which they are immersed. In order to track any behavioral difference, a detailed performance study of the solar cells and of the control board, as well as a survey of the

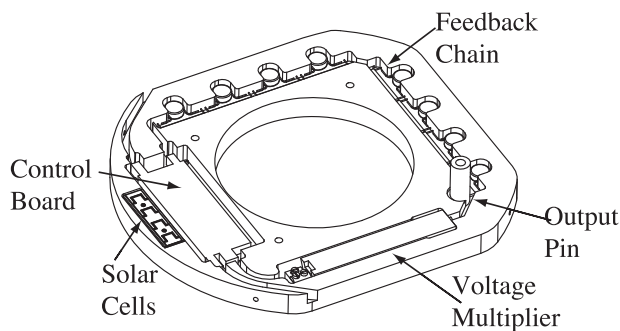


FIG. 1. Sketch of the layout of a high voltage module.

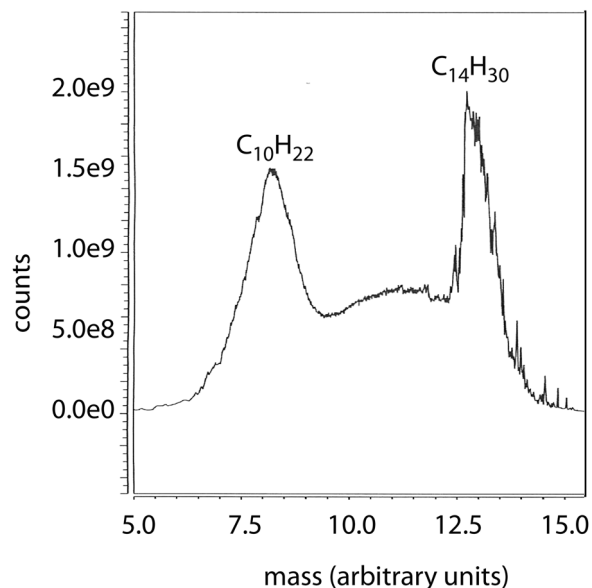


FIG. 2. Paraffin chemical composition.

global operation of the module, in both liquid and gaseous insulating environments, was carried out and will be described in the following.

It is worth noting that, having no electronics dipped in the insulator, past studies, with few exceptions (e.g., Ref. 9), were devoted more to breakdown properties of the insulating medium rather than to the actual performance of the machine within the chosen environment.

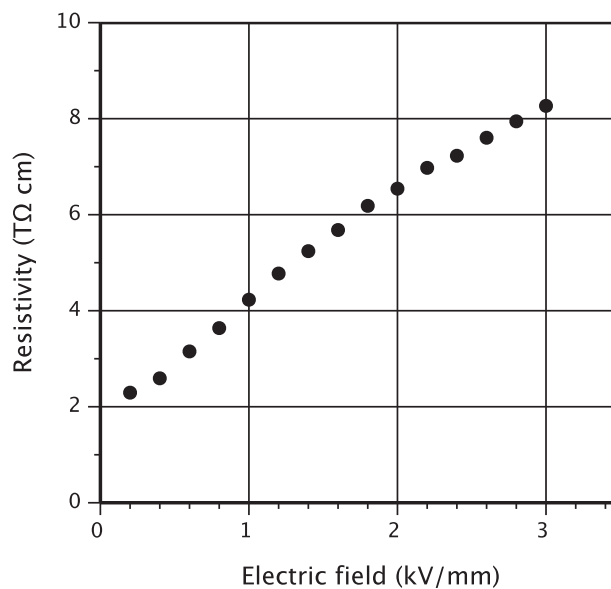


FIG. 3. Paraffin resistivity vs applied uniform electric field at $T = 298$ K.

A. Solar cells

Since the supply power is provided by laser light through optical fibers, it depends on both the laser power and the conversion efficiency of the photovoltaic cells assuming that the coupling between fiber and cell is not spoiled by the insulating medium.

Both insulating media are transparent to the selected wavelength (808 nm), but the liquid is nearly optically adapted to quartz, their refraction index being 1.42 and 1.45, respectively. The relevant consequence is that the reflection at the fiber-liquid interface is minimized, thus, slightly improving the fiber transport efficiency with respect to a fiber-gas interface.

Furthermore, the spot energy is not evenly distributed and, therefore, a certain trade-off among generated voltage, available current, and cell efficiency is unavoidable and largely dependent on the illumination conditions expressed by a filled area factor. The liquid enhances this factor because it is optically adapted and, therefore, the size of the spot on the cells is practically unchanged when exiting the fiber, while in a gas, it is enlarged by refraction. Particular care was taken to maintain always the same distance between the fiber exit and the cells in order to keep this geometric factor constant.

Besides, cell efficiency depends on its temperature:¹⁰ its value, at 808 nm laser wavelength, is about 50% and the remaining power is transferred to the surrounding environment, and heat dissipation plays an important role in the overall performance.

The control circuit uses the solar cells as a current generator, hence, the supplied current being almost constant, any power loss is detected by a drift of the electromotive force. We then investigated the cell output power loss fixing, by an active load, the absorbed current at 750 mA, which is a typical operating point of the system at the maximum high voltage. The measurement was done both for the gas and for the liquid finding a linear dependence as can be observed in Fig. 4(a). The measured power loss is $dP/dT \approx (-0.2\%) K^{-1}$, but the heat dissipation in the liquid is much more efficient and the temperature final value, obtainable from Fig. 4(b), reached after about two hours, is three times lower in the liquid than in the gas.

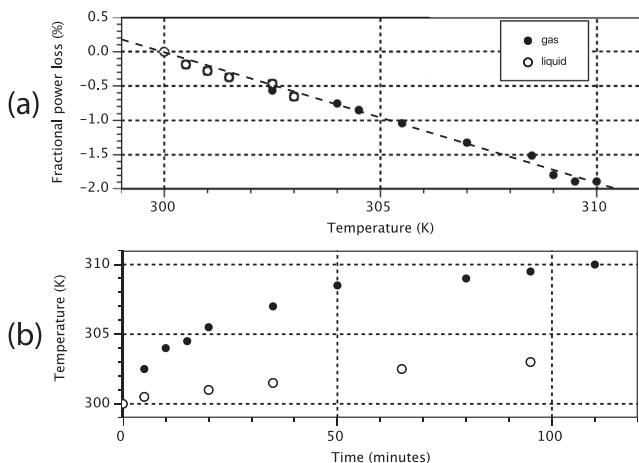


FIG. 4. (a) Output power loss as a function of cell temperature and (b) cell temperature as a function of time. Measurements were performed at 300 K environment temperature at 750 mA fixed supplied current.

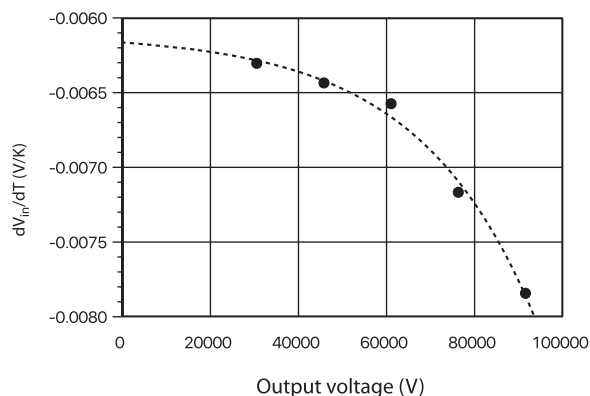


FIG. 5. Variation in the supplied voltage of the cells with temperature dV_{in}/dT vs the output voltage. The loss is evaluated for a series of four GaAs cells.

This evaluation was only partially confirmed by similar measurements performed on a fully equipped high voltage module immersed, with a resistive load, in liquid or gas during few long period acquisitions under rather different conditions. Indeed, the temperature asymptotic difference was around three times higher in gas than in liquid. Likewise, the cell output power loss rate resulted to be linear at all output voltages, but the supplied voltage variation of cells with temperature dV_{in}/dT is roughly exponentially dependent on the output voltage (Fig. 5). The open circuit voltage decrease rate of a single cell is $dV_{oc}/dT \approx 1.55 \text{ mV K}^{-1}$, compatible with the value theoretically estimated for GaAs in Ref. 10.

B. Control board

The control board performance could be influenced by the use of a liquid instead of a gas as an insulator. Indeed, parasitic currents are generated in the liquid and, since the board electronics uses

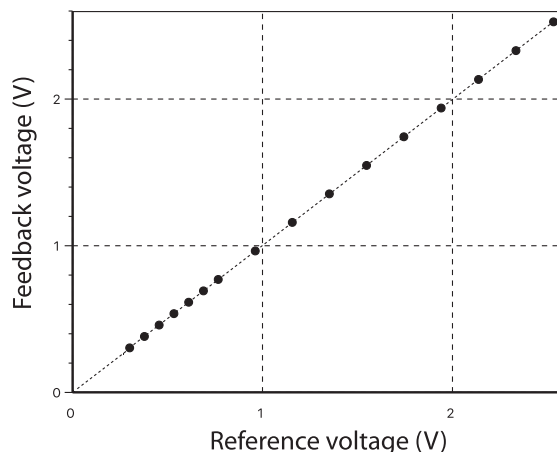


FIG. 6. Feedback voltage vs reference voltage at different set output voltages. The figure refers to measurements done with the liquid, but no significant difference was found in gas.

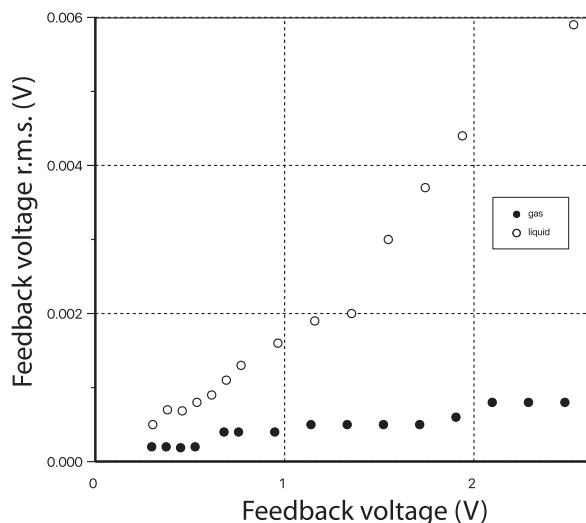


FIG. 7. Comparison of the rms between the feedback voltage in gas and liquid. Data were taken in the same working setup, i.e., with a 20 GΩ load on output.

very large values for feedback resistors, these currents could affect feedback operation and, thus, precision.

The behavior was monitored over the full range of the voltage output by comparing the feedback voltage with the reference one, which is the value programmed in a 16 bit Digital to Analog Converter (DAC) to control the high voltage output.¹¹

The resulting dependence is reported in Fig. 6 showing no significant deviation from linearity. The reference voltage at a given set value resulted completely independent of the insulating medium as well as its intrinsic noise (e.g., 0.06% rms at 30 kV output voltage), while showing a slight dependence on the temperature of about 0.09 mV K⁻¹ on the working range of 0.3 V–2.5 V (12 kV–100 kV nominal output voltage).

Difference in the behavior between liquid and gas as the insulating medium can be instead seen in Fig. 7, where an increase in the rms of the feedback voltage with the output voltage is observed.

The feedback voltage is strongly correlated with the output voltage stability and, therefore, influenced by partial discharges causing sudden voltage drops detected by the feedback chain. Its statistical dispersion is quite larger in liquid than in gas, suggesting that additional noise sources, i.e., the parasitic currents, appear in output if a liquid is used as the insulating medium.

C. Overall system performance

The main difference in the use of a gas or a liquid as insulating medium is the insurgence of a steady leakage current flowing mainly between the two electrodes embedding the module in the latter case. This current must be sustained by the power of the solar cells, thus, reducing the maximum current available for the high voltage.

A straight comparison of the amount of power required in gas and liquid is rather difficult to be obtained by direct measurements of the overall circuit power consumption due to the temperature dependence of the solar cells discussed in Sec. II A. Then, in order to allow comparisons, all the recorded data were extrapolated to the

would-be power input at a reference temperature T = 303 K, by exploiting the exponential fit shown in Fig. 5.

We analyzed the performance in gas for a few cases by changing the resistive load connected to the module output. This load adds in parallel to the always existing 40 GΩ resistive feedback chain, hence, the actual loads, R_{load} , tried were 40 GΩ (i.e., no additional load), 20 GΩ, 10.9 GΩ, and 7.5 GΩ. Only the performance with the 20 GΩ load was tested in liquid.

By analyzing these data, we could obtain the experimental power transfer function of the circuit, the device efficiency figures, and the maximum load current sustainable by the high voltage system.

The power transfer function is shown in Fig. 8: it was obtained in gas and shows a clear dependence on the load.

A deeper analysis showed that this dependence is actually both on the current drawn at the output and the output voltage V_{out} itself. Evidence of the two contributions is obtained by plotting the required input power vs the actual load current $i_{load} = V_{out}/R_{load}$ at several fixed output voltages. The resulting graphs, shown in Fig. 9, show a linear dependence of the input power on the load, which is expressed as

$$P_{in} = P_0(V_{out}) + k(V_{out})i_{load}. \quad (1)$$

The second term of the equation corresponds to the purely ohmic contribution due to R_{load} corrected by an output voltage dependent efficiency term. The fitted slope k is in fact basically the product between the output voltage and an output voltage dependent efficiency. Its value is, as a matter of fact, expressed by a step function, since it undergoes two transitions between different constant regimes around 30 kV and 65 kV output voltages. This is due to the fact that the transformer operating frequency changes around these values. The term P_0 , i.e., the power required to operate the circuit at null current load, shows instead a functional dependence on the actual output voltage (Fig. 10). The figure shows three regions where the data can be independently fitted as follows:

$$P_0 = \frac{(V_{out} - V_0)^2}{Z} + k', \quad (2)$$

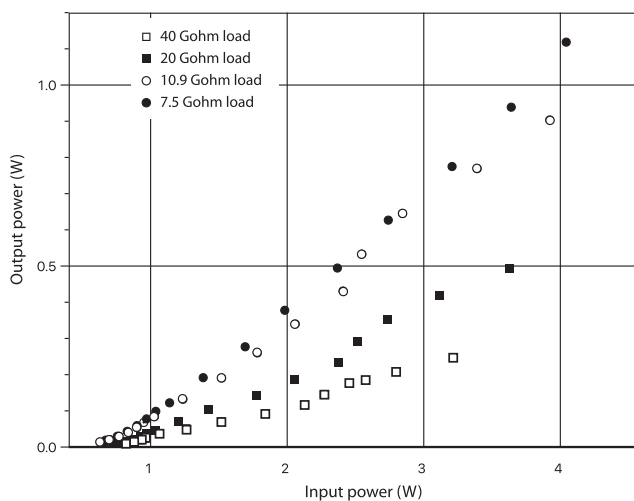


FIG. 8. Power transfer function of the control circuit for various resistive loads.

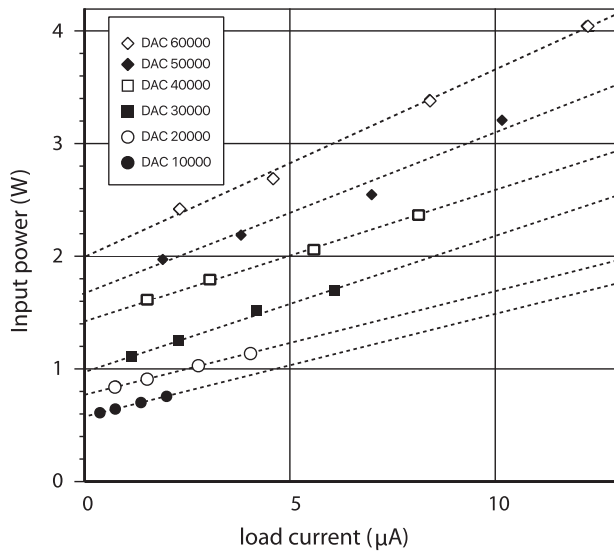


FIG. 9. Power absorbed by the control circuit vs the load current for various resistive loads at different output voltages. The lines are linear fits to the data: the step transitions of the slope at the DAC set value greater than 20 000 and 40 000, characterizing three different working regimes, are evident from the graph. The points of each series of the DAC set value correspond to the four resistive loads decreasing while going toward right on the graph. Only data corresponding to a few DAC set values are shown for the sake of clarity.

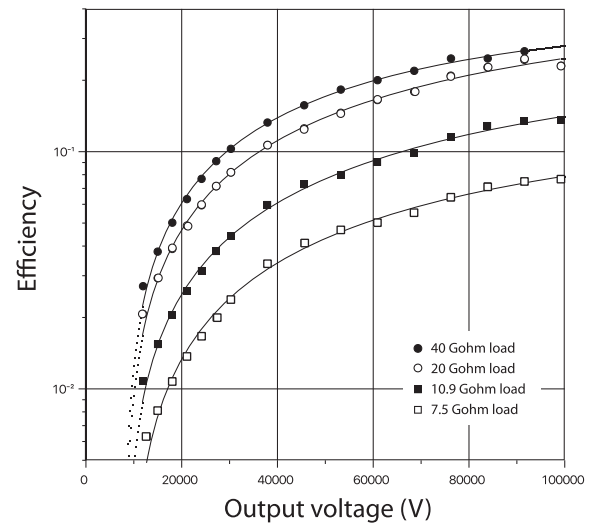


FIG. 11. Efficiency of the control circuit for several resistive loads vs the measured output voltage. The lines are drawn just to guide the eye.

where Z is the impedance of the control circuit, excluding R_{load} , confirming that the board is working in three different regimes, depending on the required output voltage.

Some work is in progress in order to stabilize the control circuit avoiding these transitions while maintaining minimal possible power consumption.

The transfer function information could also be transformed into an efficiency figure by plotting the efficiency $e = P_{out}/P_{in}$ in Fig. 11. The efficiency is increasing with the required output voltage because the excess power dissipated on the cells is decreasing. The same argument holds at fixed output voltage if a lower resistive load, i.e., a greater load current, is sustained on output because the power P_0 required to operate the circuit at that given voltage is always the same.

When the high voltage generator is immersed in the liquid, a leakage current adds to the one flowing in the resistive load.

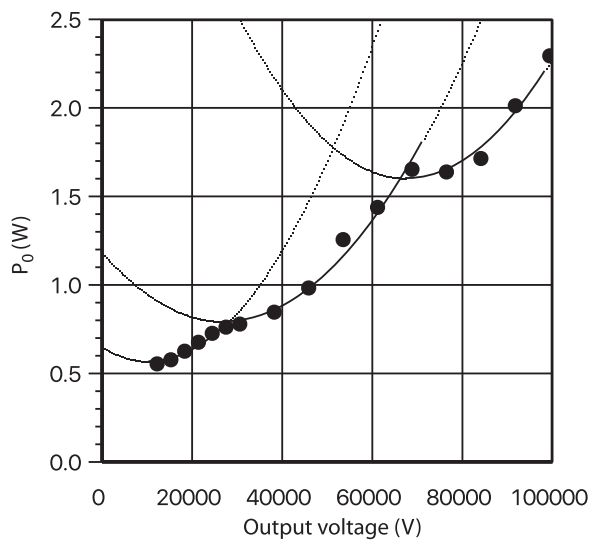


FIG. 10. Power absorbed by the control circuit at the null output current vs the set output voltage. The lines are parabolic fits of the equation $(V - V_0)^2/Z + k'$.

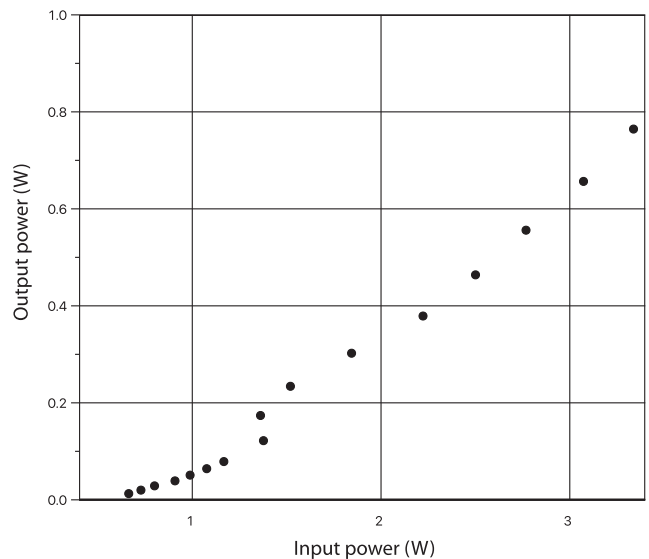


FIG. 12. Power transfer function of the control circuit when immersed in liquid with a 40 GΩ resistive load on output.

The leakage current was directly measured⁷ and found to be described as

$$i_{leak} = \frac{V_{out}}{R_0(1 + \alpha V_{out})}, \quad (3)$$

which is measured in amperes and V_{out} is the output voltage in volts, where the parameters $R_0 = 25.74 \text{ G}\Omega$ and $\alpha = 5.56 \times 10^{-6} \text{ V}^{-1}$ are obtained by the fit.

The overall load current can then be computed, thus, providing the transfer function in the measured case when the resistive load is $20 \text{ G}\Omega$. Its behavior, displayed in Fig. 12, clearly shows the transition of the circuit between the two operating regimes occurring around 30 kV output voltage. The behavior is non-ohmic; thus, the resistance is voltage dependent and can be obtained from Eq. (3). Including this contribution, the expected range of the total resistive load is between $16 \text{ G}\Omega$ and $20 \text{ G}\Omega$: as expected by the comparison with Fig. 8, the transfer function is in between the ones measured in gas with the $10.9 \text{ G}\Omega$ and the $20 \text{ G}\Omega$ loads.

The average system performance was unchanged with respect to the gas. Figure 13(a) reports the linearity of the measured output voltage vs the value set on the DAC. The residuals of the fit [Fig. 13(b)] to the points measured at low voltage show a deviation from linearity compatible with the derating of the resistors of the divider used for measurements, which can be fixed by calibration.

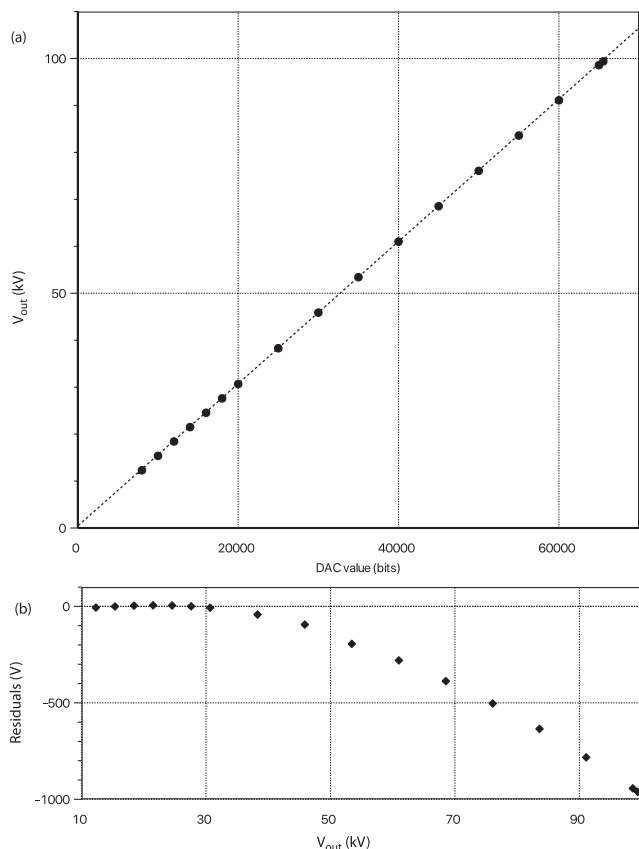


FIG. 13. (a) Linearity of the high voltage system when immersed in liquid; (b) residuals of the line fit only to low voltage data (DAC value lower than 20 000). The measurements were done in liquid, and no significant difference was found in gas.

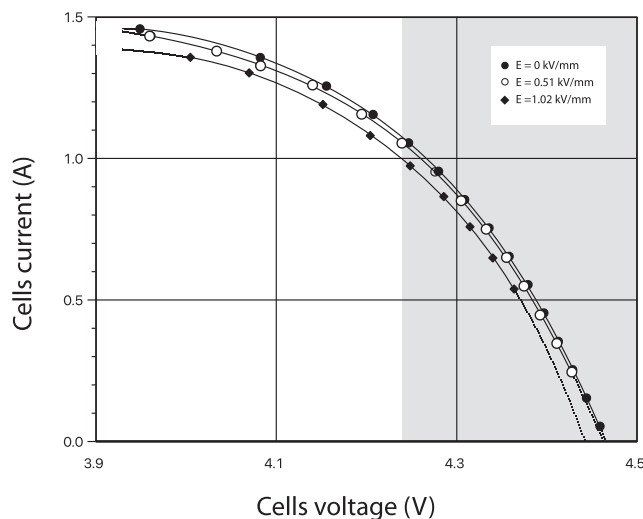


FIG. 14. Volt–ampere characteristic of the series of four cells under operating conditions. A slight dependence on the external electric field is seen: the power supplied by the solar cells is decreasing with the field. The gray area highlights the working range of the experimentally determined system.

The volt–ampere characteristic of the power cell series, referred at $T = 303 \text{ K}$ using the fit of Fig. 5, determined in gas under operating conditions, is shown in Fig. 14. The curve shows a slight dependence on the intense electric field in which the solar cells are immersed: the current supplied by the cells at a given voltage decreases by about 5%–6% from 0 V to 100 kV output voltage. This means that the overall input power available is decreasing with high voltage. The shaded area in the figure reports the experimentally available working range of the system. In particular, the lower limit ($V_{cells} \approx 4.25 \text{ V}$ and $I_{cells} \approx 1 \text{ A}$, but the figure is temperature dependent) was found at about $12 \mu\text{A}$ output current at 100 kV output voltage. This value could be roughly considered the nominal limit of the current sustainable by the system at 100 kV, although the control board can still work at an input voltage as low as 3.3 V, thus, slightly extending the actual load current range. Considering that $2.5 \mu\text{A}$ current is always absorbed by the feedback voltage divider, the maximum load current in gas is about $9.5 \mu\text{A}$. Since, while operating in liquid, an additional leakage current of about $2.5 \mu\text{A}$, computed using Eq. (3), appears; this limit is reduced to about $7 \mu\text{A}$ if the insulation is ensured by liquid. Of course, operating at lower voltage, a higher load current could be sustained.

III. CONCLUSIONS

The tests performed on a liquid dielectric for a very high voltage module show that it is a valid alternative to the usual high pressure gas electrical insulation.

A detailed analysis of the system performance revealed that the only important issue with respect to the gas is the appearance of a relevant leakage current that must be sustained by the device. This current causes considerable efficiency reduction and increasing noise in the device with respect to the gas case. It is worth considering that the detection of increasing noise is an evident signal

of the prodromes of the establishment of a discharge regime. The control board allows a continuous monitoring of this parameter that could be used in order to protect the system from destructive sparks.

The detected problems should be considered against the clear safety advantage of operating at the atmospheric pressure: the trade-off between safety and efficiency should be carefully evaluated.

ACKNOWLEDGMENTS

This work was funded by the Padua University in the framework of the Departmental Research, Grant No. BIRD172341/2017, and by the Istituto Nazionale di Fisica Nucleare in the framework of the G5/MOPEA project.

The authors thank Dr. Carlo Scian of the Physics and Astronomy Department of the Padova University for the refraction index measurements and Professor Paolo Pastore of the Chemistry Department of Padua University for the paraffin composition analysis.

DATA AVAILABILITY

The data that support the findings of this study are available from the corresponding author upon reasonable request.

REFERENCES

- ¹P. Antonini, E. Borsato, G. Carugno, M. Pegoraro, and P. Zotto, *Rev. Sci. Instrum.* **84**, 024701 (2013).
- ²P. Antonini, A. Benato, E. Borsato, G. Carugno, R. Gobbo, F. Montecassiano, M. Pegoraro, G. Pesavento, M. Zago, and P. Zotto, *Rev. Sci. Instrum.* **88**, 025113 (2017).
- ³R. J. Adler and R. J. Richter-Sand, "Advances in the development of the nested high voltage generator," in *Proceedings of International Conference on Particle Accelerators* (SPIE, 1993), Vol. 2, pp. 1306–1308.
- ⁴S. S. Gjerde and T. M. Undeland, *Energy Procedia* **24**, 68–75 (2012).
- ⁵K. Xie, A.-F. Huang, X.-P. Li, S.-Z. Guo, and H.-L. Zhang, *Rev. Sci. Instrum.* **86**, 044707 (2017).
- ⁶E. Gockenbach and H. Borsi, "New insulating liquids for high voltage apparatus," in *2008 IEEE International Conference on Dielectric Liquids* (IEEE, 2008), pp. 1–4.
- ⁷P. Antonini, E. Borsato, G. Carugno, F. Dal Corso, A. Facco, C. Fanin, R. Gobbo, L. La Torre, F. Montecassiano, M. Pegoraro *et al.*, "Studies for the use of a dielectric liquid as insulator in a wireless high voltage generator," in *IEEE 20th International Conference on Dielectric Liquids (ICDL)* (IEEE, 2019).
- ⁸A. W. Bright and B. Makin, *Contemp. Phys.* **10**, 331–353 (1969).
- ⁹N. J. Felici, *Electron. Power* **11**, 169–171 (1965).
- ¹⁰P. Singh and N. M. Ravindra, *Sol. Energy Mater. Sol. Cells* **101**, 36–45 (2012).
- ¹¹Measurements reported hereafter refer to the following DAC set values: 8000, 10 000, 12 000, 14 000, 16 000, 18 000, 20 000, 25 000, 30 000, 35 000, 40 000, 50 000, 55 000, 60 000, and 65 000. The corresponding output voltage (in volt) is obtained by multiplying the DAC value (in bits) by 1.529. The DAC voltage V_{ref} range is 0 V–2.5 V thus $V_{out} = 40\,000 \times V_{ref}$.